

**FISSION OF SWIFT HEAVY IONS AND
PARTICLE EVAPORATION
IN
NUCLEAR TRACK DETECTORS**

Jolly Raju

A thesis submitted in partial fulfilment of the requirements

for the degree of

DOCTOR OF PHILOSOPHY

in

Chemistry

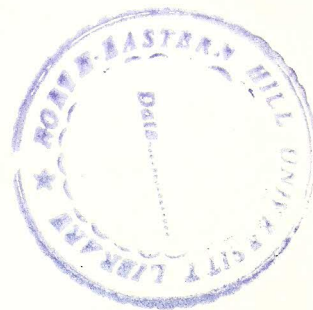


Department of Chemistry

NORTH-EASTERN HILL UNIVERSITY

Shillong- 793 003 (India)

1994



DEDICATED

TO

MY PARENTS



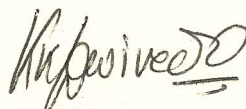
North-Eastern Hill University

Bijni Complex, Bhagyakul
Shillong - 793 003 (Meghalaya), India.

Dr. K.K. Dwivedi,
Reader in Chemistry.

CERTIFICATE I

This is to certify that the thesis entitled "FISSION OF SWIFT HEAVY IONS AND PARTICLE EVAPORATION IN NUCLEAR TRACK DETECTORS" submitted by Mr. Jolly Raju for the Degree of Doctor of Philosophy of the North-Eastern Hill University, Shillong, INDIA, embodies the records of original investigations carried out by him under my supervision. He has been duly registered and the thesis presented is worthy of being considered for the award of Ph.D. This work has not been submitted elsewhere for a degree.


K. K. Dwivedi

Thesis Supervisor

North-Eastern Hill University


Bijni Complex, Bhagyakul
Shillong - 793 003 (Meghalaya), India.

Prof. S. N. Bhat
Head,
Department of Chemistry.

CERTIFICATE II

This is to certify that Mr. Jolly Raju has satisfactorily completed the following Pre-Ph.D. courses.

<u>Courses</u>	<u>Grades</u>
1. Basic German Language	O
2. Numerical Methods with applications to computer programming.	O
3. Applications of Nuclear and Radiochemistry.	A
4. Solid State Chemistry.	A


Prof. S.N. Bhat.
HEAD
Department of Chemistry
North Eastern Hill University
Shillong-793 003

ACKNOWLEDGEMENTS

I express my gratitude to my guide (sir) **Dr. K.K. Dwivedi**, who has not only guided me all along the course of this work, but also was a constant source of inspiration. It was he who had introduced me to this field of "interaction of energetic heavy ions with solids" and its branching area of the fascinating "fork-like events".

I extend my thanks to **Dr. G. Fiedler** and **E. Reichwein** (Justus - Liebig Universität, Giessen, Germany) for certain result oriented discussions at the initial stages of this work.

Also **Prof. R. Brandt** and **Dr. P. Vater** (Kernchemie, Philipps - Universität, Marburg, Germany) for fruitful discussions and **Prof. S.S. Kapoor** (Director, Physics, electronics and instrumentation group, BARC, Bombay, India) for certain effective suggestions during the course of the work.

Thanks are due to **Dr. B. Patro** and **Mr. Nobin Terang** for their help and companionship during the later stages of this work, which helped me to give the present look to the manuscript. Also **the faculty members**, Department of Mathematics, NEHU for allowing me to use their computer for the same.

I thank **Drs. R. Spohr, J. Vetter and C. Trautmann** of GSI, Darmstadt for their help in heavy ion irradiations at UNILAC.

A financial assistance in the form of NEHU (UGC) fellowship (under UGC/CSIR, (NET)) is gratefully acknowledged. Another financial assistance in the form of travel grant by CSIR, New-Delhi, India, to attend the 16th International Conference on Nuclear Tracks in Solids", at Beijing, China, held during Sept. 7-11, '92 is also acknowledged.

I thank **Dr. D.W. Fink** of Hahn-Meitner Institute, Berlin and **Prof. L.T. Chadderton** of Australian National University, Canberra for productive discussions during my stay at Beijing.

I also thank **Mr. Shivaprakashan** and **Mr. Vijayan** for typing of the manuscript.

I thank my teachers for their inspirations.

Also my friends **Vimal, Vidya, Rajesh, Ashraf, Donga, Mazami** for their help.

My thanks also are due to **Mrs. Rekha Dwivedi, Tinu, and Vinni** for their love and care.

My parents for always encouraging me to take up new challenges, my sisters (Manju and Anju) for the care and my brother (Manoj) who offered me a helping hand in every possible way, he could.

Jolly Raju

CONTENTS

	Page
STATEMENT	iii
CERTIFICATE I	iv
CERTIFICATE II	v
ACKNOWLEDGEMENTS	vi
CONTENTS	viii
LIST OF TABLES	xi
LIST OF FIGURES	xv
CHAPTER I INTRODUCTION	1
CHAPTER II THEORETICAL ASPECTS	
II.1 Geometrical aspect of an event	10
II.1.1 Determination of real lengths of the prongs.	10
II.1.2 Determination of real opening angles	16
II.1.3 Determination of tilting angles	20
II.1.4 Crosscheck for the derived equations	23
II.2 Range energy calibrations	26
II.3 The program 'TRANSCORD'	26
II.4 The program 'HIFISS'	28
II.4.1 Total mass of fragments	32
II.4.2 The Q-value	35
II.4.3 Relative velocity of the fragments	37

	Page
II.4.4 Total opening angle in Laboratory and centre of mass system	37
II.4.5 Data test for the program 'HIFISS'	39
II.5 Differential and total cross-section	42
II.6 Analysis of the third prong	42
CHAPTER III EXPERIMENTAL PROCEDURE	48
III.1 Selection of detectors	48
III.2 Preparation of detectors and irradiations	49
III.3 Chemical processing	51
III.4 Observation and scanning	54
III.4.1 Measurement of various parameters	54
III.4.2 Determination of track Density	57
III.4.3 Determination of energy of the projectiles	58
III.5 Calibration of detectors	58
III.6 Error analysis	63
III.6.1 Experimental errors	63
III.6.2 Errors in the derived quantities	68
III.6.3 Errors in the different kinematic variables	68
CHAPTER IV RESULTS AND DISCUSSION	70
IV.1 Statistics of events	70
IV.2 Differential and total cross-section	74
IV.3 Total mass of fragments	89
IV.4 The Q-values of the nuclear reactions	95
IV.5 Fragment mass distributions	108

	Page
IV.6 Relative velocity of fragments	113
IV.7 Total opening angle in laboratory system	113
IV.8 Total opening angle in centre of mass system	125
IV.9 Analysis of the third prong.	125
CHAPTER V CONCLUSION AND FUTURE PERSPECTIVES	140
REFERENCES	144
APPENDIX A COMPUTER CODE 'TRANSCORD'	156
APPENDIX B COMPUTER CODE 'HIFISS'	161
LIST OF PUBLICATIONS	172

LIST OF TABLES

<u>Table No.</u>	<u>Contents</u>	<u>Page</u>
II.1	Summary of the equations derived in order to determine the values of different parameters of an event.	25
II.2	Q-Values calculated from Viola systematics for fission of $^{238}\text{U} + (\text{H}, \text{C}, \text{O})$ and $^{209}\text{Bi} (\text{H}, \text{C}, \text{O})$.	36
II.3	Values of different parameters of the artificial events for testing the program 'HIFISS'.	40
II.4	Output values obtained from the program 'HIFISS' for the artificial events.	41
II.5	Summary of equations derived to determine different parameters of the third prong.	45
II.6	Systematic approach to analyze the directional behaviour of the third prong along with the angle with respect to the beam direction.	47
III.1	Important properties of CR-39 and Makrofol-E.	50
III.2	Specifications of Irradiations carried out.	52

<u>Table No.</u>	<u>Contents</u>	<u>Page</u>
III.3	An account on the suitable etchants and the etching conditions found and used for the two detectors.	53
III.4	Best sets of coefficients derived for track length energy calibrations of ^{238}U in CR-39.	60
III.5	Best sets of coefficients derived for track length energy calibrations of ^{238}U in Makrofol-E.	61
III.6	Best sets of coefficients derived for track length energy calibrations of ^{209}Bi in CR-39 and Makrofol-E.	62
III.7	Best set of coefficients for mass dependent range-velocity calibration for ^{238}U in CR-39.	64
III.8	Best set of coefficients for mass dependent range-velocity calibration for ^{238}U in Makrofol-E.	65
III.9	Best set of coefficients for mass dependent range-velocity calibration for ^{209}Bi in CR-39.	66
III.10	Best set of coefficients for mass dependent range-velocity calibration for ^{209}Bi in Makrofol-E.	67
III.11	Errors in the values of real parameters due to measurement inaccuracies.	69
IV.1	Statistics of events.	71 — 73

<u>Table No.</u>	<u>Contents</u>	<u>Page</u>
IV.2	Differential cross-sections corresponding to resonance peaks for ^{238}U in CR-39.	80
IV.3	Differential cross-sections corresponding to resonance peaks for ^{238}U in Makrofol-E.	85
IV.4	Differential cross-sections corresponding to resonance peaks for ^{209}Bi in CR-39 and Makrofol-E.	88
IV.5	Total cross-sections for ^{238}U in CR-39 at different initial energies of the projectile.	90
IV.6	Total cross-sections for ^{238}U in Makrofol-E at different initial energies of the projectile.	91
IV.7	Total cross-sections for ^{209}Bi of 13.0 MeV/u in CR-39 and Makrofol-E.	94
IV.8	Most probable total mass of fragments for ^{238}U of different initial energies in CR-39 and Makrofol-E.	100
IV.9	Most probable total mass of fragments for 13.0 MeV/u ^{209}Bi in CR-39 and Makrofol-E.	101
IV.10	Most probable Q-Values for ^{238}U of different initial energies in CR-39 and Makrofol-E.	106
IV.11	Most probable Q-Values for 13.0 MeV/u ^{209}Bi in CR-39 and Makrofol-E.	107

<u>Table No.</u>	<u>Contents</u>	<u>Page</u>
IV.12	Most probable relative velocity of fragments for ^{238}U of different initial energies in CR-39 and Makrofol-E.	118
IV.13	Most probable relative velocity for 13.0 MeV/u ^{209}Bi in CR-39 and Makrofol-E.	119
IV.14	Values of measured and derived parameters of the third prongs for ^{238}U in CR-39.	139

LIST OF FIGURES

<u>Figure</u>		<u>Page</u>
I.1	A photomicrograph of a fork-like event in CR-39. The CR-39 was irradiated to 15.2 MeV/u ^{238}U ions.	3
I.2	A photomicrograph of two events in CR-39. The detector was irradiated to 16.3 MeV/u ^{238}U projectiles [38].	4
I.3	Another photomicrograph of a fork like event with the third prong at the point of scission in CR-39. The CR-39 was irradiated to 16.4 MeV/u ^{238}U ions.	5
II.1	Representation of a fork like event and its projection on observation (x,y) plane.	11
II.2 (a)	A typical view of the two planes: plane of the event and plane of observation.	12
II.2 (b)	A view of an event showing different parameters in its own plane.	13

<u>Figure</u>		<u>Page</u>
II.2(c)	Projection of an event on the observation plane (x,y) showing different projected parameters.	14
II.3	A line diagram showing the dip angles and depth of the prong tips with respect to a reference plane parallel to the observation plane containing the scission point O.	15
II.4	Diagram showing the two planes containing the prongs 'A' and 'B' as a result of tilting from the plane 1 by angles δ_A and δ_B respectively and the bending angle β between these planes.	17
II.5	A diagram to illustrate the tilting of prongs, resulting in to the formation of two co-axial syn-apical cones.	18
II.6	End-on-view showing loci of prong tips in the form of two concentric circles. The parameters shown here are used for the determination of the real opening angles θ_A and θ_B .	19
II.7	A line diagram of the planes due to the tilting of the prongs in order to derive the tilting angles (δ_A and δ_B).	21
II.8	A flow chart of the program 'TRANSCORD'. The input and output variables are also stated.	27
II.9	Representation of a 'BINARY TREE' in the binary search algorithm.	29

<u>Figure</u>		<u>Page</u>
II.10	A diagram to explain the dynamics of fission process in terms of different momentum components.	31
II.11	A flow chart of the program 'HIFISS'. The input and output variables are also stated.	33
II.12	A flow chart showing the different interactive subroutines and functions of the program 'HIFISS'.	34
II.13	A diagram to explain the different velocity vectors for the determination of relative velocity and the total opening angle in the centre of mass system.	38
II.14	Line diagrams showing an event with the third prong. (a) Top view (xy -plane). (b) Side view (xz-plane) . Different parameters are also indicated.	44
III.1	A line diagram of an event with different projected and real parameters.	55
III.2	An enlarged view of the angle measuring device.	56
IV.1	Plot of Number of events at different pre-fission energies for 16.4 MeV/u ^{238}U in CR-39. Resonance peaks observed at a) 7.0 MeV/u, b) 9.4 MeV/u, c) 11.8 MeV/u, d) 14.2 MeV/u.	75

<u>Figure</u>		<u>Page</u>
IV.2	Plot of number of events at different pre-fission energies for 15.2 MeV/u ^{238}U in CR - 39. Resonance peaks at a) 7.0 MeV/u; b) 9.4 MeV/u; c) 11.8 MeV/u; d) 14.2 MeV/u are shown.	76
IV.3	Plot of number of events at different pre-fission energies for 14.0 MeV/u ^{238}U in CR- 39. a) 7.0 MeV/u; b) 9.4 MeV/u; c) 11.8 MeV/u are the positions of the resonance peaks.	77
IV.4	Plot of number of events at different pre-fission energies for 13.0 MeV/u ^{238}U in CR - 39. Resonance peaks are observed at a) 7.0 MeV/u; b) 9.4 MeV/u; c) 11.8 MeV/u.	78
IV.5	Plot of number of events at different pre-fission energies for 11.3 MeV/u ^{238}U in CR - 39. Two resonance peaks shown are at a) 7.0 MeV/u; b) 9.4 MeV/u.	79
IV.6	Plot of number of events occurring at different pre-fission energies for 17.2 MeV/u ^{238}U in Makrofol-E. Resonance peaks observed at energies a) 7.0 MeV/u, b) 9.4 MeV/u, c) 11.8 MeV/u, d) 14.2 MeV/u.	81
IV.7	Plot of number of events occurring at different pre-fission energies for 16.0 MeV/u ^{238}U in Makrofol-E. Resonance peaks observed at energies a) 7.0 MeV/u, b) 9.4 MeV/u, c) 11.8 MeV/u, d) 14.2 MeV/u.	82

<u>Figure</u>		<u>Page</u>
IV.8	Plot of number of events occurring at different pre-fission energies for 14.0 MeV/u ^{238}U in Makrofol-E. Resonance peaks observed at energies a) 7.0 MeV/u, b) 9.4 MeV/u, c) 11.8 MeV/u.	83
IV.9	Plot of number of events occurring at different pre-fission energies for 12.4 MeV/u ^{238}U in Makrofol-E. Resonance peaks observed at energies a) 7.0 MeV/u, b) 9.4 MeV/u, c) 11.8 MeV/u.	84
IV.10	Plot of number of events occurring at different pre-fission energies for 13.0 MeV/u ^{209}Bi in CR-39.	86
IV.11	Plot of number of events occurring at different pre-fission energies for 13.0 MeV/u ^{209}Bi in Makrofol-E.	87
IV.12	Excitation function plot for ^{238}U in CR-39.	92
IV.13	Excitation function plot for ^{238}U in Makrofol-E	93
IV.14	Total mass of fragments distribution for 14.0 MeV/u ^{238}U in CR-39.	96
IV.15	Total mass of fragments distribution for 16.0 MeV/u ^{238}U in CR - 39.	97
IV.16	Total mass of fragments distribution for 13.0 MeV/u ^{209}Bi in CR-39.	98

<u>Figure</u>		<u>Page</u>
IV.17	Total mass of fragments distribution for 13.0 MeV/u ^{209}Bi in Makrofol-E.	99
IV.18	Q-value distribution for 16.4 MeV/u ^{238}U in CR-39.	102
IV.19	Q-value distribution for 17.2 MeV/u ^{238}U in Makrofol-E	103
IV.20	Q-value distribution for 13.0 MeV/u ^{209}Bi in Makrofol-E	104
IV.21	Q-value distribution for 13.0 MeV/u ^{209}Bi in Makrofol-E	105
IV.22	Fragment mass distribution for ^{238}U in CR-39.	109
IV.23	Fragment mass distribution for ^{238}U in Makrofol-E.	110
IV.24	Fragment mass distribution for ^{209}Bi in CR-39.	111
IV.25	Fragment mass distribution for ^{209}Bi in Makrofol-E.	112
IV.26	Relative velocity distribution for 16.4 MeV/u ^{238}U in CR-39.	114
IV.27	Relative velocity distribution for 17.2 MeV/u ^{238}U in Makrofol-E.	115

<u>Figure</u>		<u>Page</u>
IV.28	Relative velocity distribution for 13.0 MeV/u ^{209}Bi in CR-39.	116
IV.29	Relative velocity distribution for 13.0 MeV/u ^{209}Bi in Makrofol-E.	117
IV.30	Plot of total opening angle in laboratory system at different pre-fission energies for ^{238}U in CR-39 a) 16.4 MeV/u, b) 14.0 MeV/u, c) 13.0 MeV/u.	120 122
IV.31	Total opening angle in laboratory system at different pre-fission energies for ^{238}U in Makrofol-E a) 17.2 MeV/u, b) 16.0 MeV/u.	123 124
IV.32	Plot of total opening angle in laboratory system for 13.0 MeV/u ^{209}Bi in CR-39.	126
IV.33	Plot of total opening angle in laboratory system for 13.0 MeV/u ^{209}Bi in Makrofol-E.	127
IV.34	Plot of total opening angle in centre of mass system for ^{238}U in CR-39. a) 16.4 MeV/u, b) 14.0 MeV/u, c) 13.0 MeV/u.	128 129 130
IV.35	Plot of total opening angle in centre of mass system for ^{238}U in Makrofol-E. a) 17.2 MeV/u, b) 16.0 MeV/u.	131 132
IV.36	Plot of total opening angle in centre of mass system for ^{209}Bi in CR-39.	133

Figure

Page

IV.37	Plot of total opening angle in centre of mass system for ^{209}Bi in Makrofol-E.	134
IV.38	Plot of number of events as a function of centre of mass energy ($^{238}\text{U} + ^{12}\text{C}$) for ^{238}U of 16.4 MeV/u in CR -39.	136
IV.39	A photomicrograph of the ninth event of Table IV.14.	137
V.I	Two photomicrographs of the same event showing the multiparticle emission in CR-39 irradiated to 15.2 MeV/u ^{238}U .	143

CHAPTER I

INTRODUCTION

CHAPTER I

INTRODUCTION

Solid State Nuclear Track Detectors commonly abbreviated as SSNTDs have been applied [1,2,3] in a wide spectrum of scientific and technical fields. The utility of this versatile technique ranges from nuclear science and engineering to cosmic ray astrophysics and from geology, archeology and sub-oceanic geophysics to lunar science and meteorites [4,5,6]. Right from the development of this track technique, its versatility has been exploited in anthropology [7], geochronology [8], environmental sciences [9], space research [10], superfluidity [11,12], lithography [13], dosimetry [14], medical research [15], study of heavy ion nuclear reactions [16-19], multifragmentation of the projectile [20, 21, 22], particle identification [23, 24], search for magnetic monopoles [25, 26], discovery of super heavy elements [27], exotic decay modes of heavy nuclei [28,29].

This has been possible due to certain advantageous features of these track detectors such as the easy availability, inexpensive and a large choice of detectors ranging from organic polymers to inorganic crystals. At times the detectors are available naturally at the site of interest. The inherent characteristics of these detectors are that they have excellent resolution for mass, charge and energy [30] within the boundaries of experimental errors.

The technique too does not require heavy budget equipments. Besides these, the detectors carry a permanent record of the radiation damage to which they were exposed. Moreover the detectors can withstand a large dose of lighter particles and low ionizing radiation.

During the past few years measurement of energy-loss of heavy ions in different elemental and complex media using nuclear track technique has been carried out [31,32]. The involvement was also in the characterisation and calibration [33,34] of different track detectors for a purposeful utility of these detectors in different fields. Different studies to explore more on the track formation mechanism were also carried out [35,36,37]. For the mentioned studies confinement was to the linear tracks i.e the enlarged damage trails of the trajectories of energetic heavy ions in the detector matrix created by chemical processing.

Fig. I.1 is a photomicrograph of a fork-like event in CR-39 irradiated to ^{238}U ions of 15.2 MeV/u. In 1988 Dwivedi et.al. [38] reported the observation of fork – like events in CR-39 irradiated to ^{238}U ions of 1.6 GeV. A photomicrograph of two events from their report is shown in **Fig. I.2**. As the different experiments in CR-39, Makrofol-E, Cellulose Nitrate and Mica irradiated to ^{208}Pb , ^{209}Bi and ^{238}U were in progress, similar fork like events were encountered. Fork-like events with a third prong of comparatively shorter length have been observed at the point of bifurcation (fission) for ^{238}U in CR-39 (**Fig. I.3**). Having observed such fork like events a few fundamental queries, which needed explanations were : (i) Definitely the scission of the projectile takes place in the forward hemisphere but is there a possibility of fusion with the nuclei of the atoms constituting the detector matrix, (ii) A suitable reason for the existence of the third prong. The probable answers to these queries can be sought after determining the masses in the exit channels, the angular distributions of the fragments, Q-Value of the reactions, the relative velocity of fragments and total opening angle in the laboratory and center of mass systems.

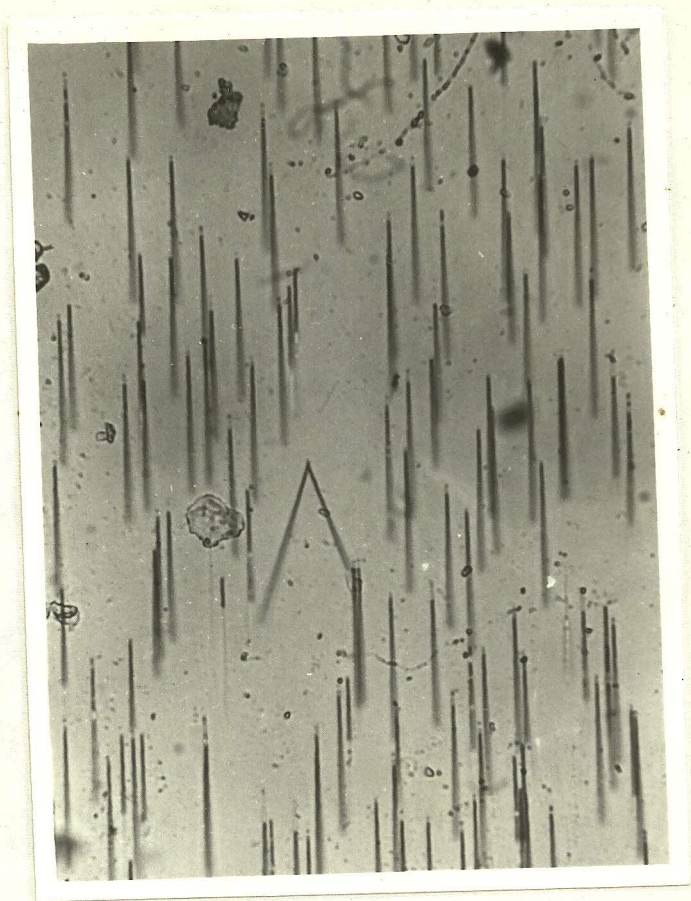


Fig. I.1 A photomicrograph of a fork-like event in CR-39 irradiated to 15.2 MeV/u ^{238}U .

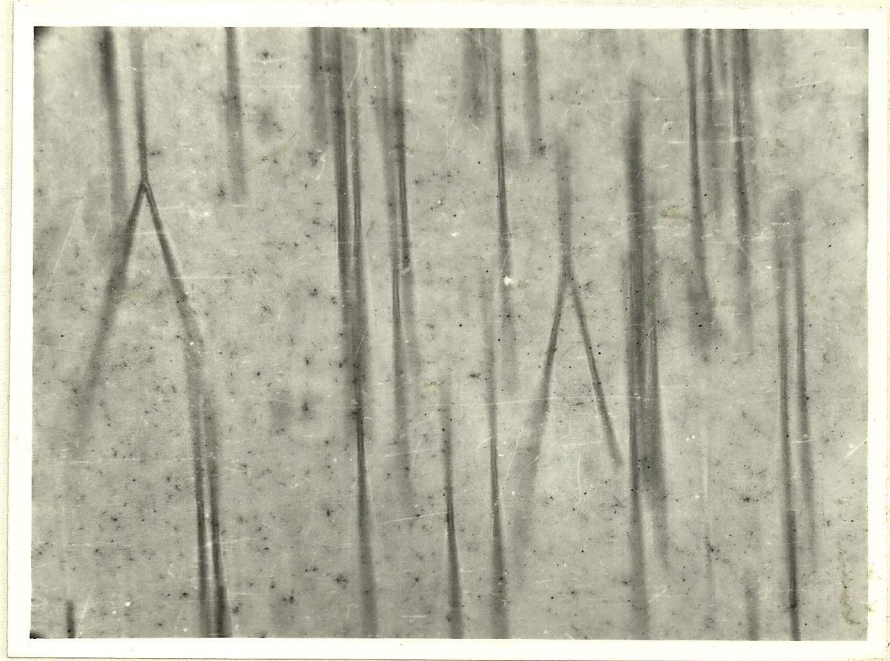


Fig. I.2 A photomicrograph; two events from Dwivedi and Fiedler [38] in CR-39 irradiated to 16.3 MeV/u ^{238}U ions.

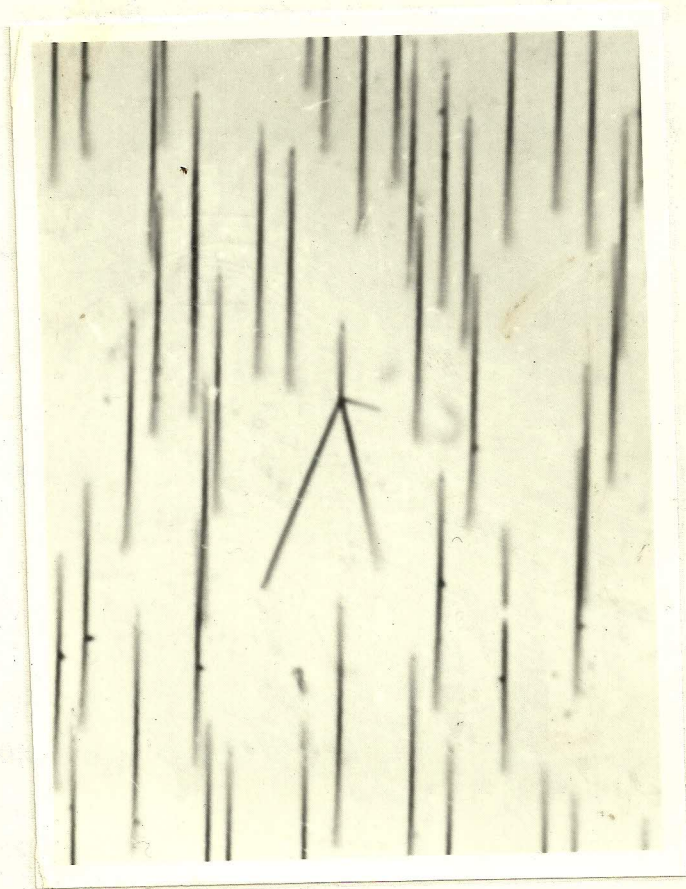


Fig. I.3 A photomicrograph of a fork-like event with the third prong at the point of scission in CR-39. The CR-39 was irradiated to 16.4 MeV/u ^{238}U ions.

On the way to seek the answers to the queries by determining different kinematic variables of the events few barriers too were encountered. They are:

(i) Deriving the real values of different parameters of the prongs from the microscopically observed projected images. The different parameters of the events to be derived are the real lengths of the prongs, the real opening angles with respect to the beam direction and the energy of the projectile at the scission point.

(ii) Analysing each event in terms of the masses of the fragments in the exit channels and other kinematic variables such as the Q-value of the reaction, relative velocity of the fragments, opening angle in the laboratory and centre of mass systems.

(iii) Developing a systematic approach to study the third prongs in terms their actual track lengths and distribution around the axis considered along the trajectory of the projectile.

In an attempt to search the solutions for the above queries along with overcoming the barriers, a 4π geometry technique has been developed for the analysis of these fork-like events. It consists of a geometrical approach followed by computational analysis. The geometrical part takes care of the first barrier while the computational part tackles the second. A systematic approach has been developed to analyze the third prongs in terms of their true track lengths, direction of existence and also the angle with respect to the beam direction. This technique is advantageous over other techniques of radiation measurement as each individual event is registered as a permanent record in the detector matrix. Hence multiple measurements of the same event can be carried out even after few years of its occurrence. It also offers the recording of spatially distributed particles in 4π geometry unlike any other conventional 2π detection system.

A description of the subsequent chapters are as follows:

(i) **Chapter II** deals with the theoretical aspects of analysis of the events: geometrical approach followed by computational. In section II.1 the geometrical aspect of the event is discussed where the derivations of different real parameters of an event from the projected parameters have been accomplished. Section II.2 deals with the methods to construct range-energy calibrations needed to calculate pre-fission energy of the projectiles. In section II.3, the logic and the functions of the program 'TRANSCORD' developed for the first step of analysis are described. The second step of analysis done with the help of the application program 'HIFISS' is explained in section II.4 along with the logic used. The trivialities involved in the computation of different kinematical variables along with the mathematical equations used for the purpose are discussed in this chapter. The systematic steps undertaken to study the third prongs have also been explained.

(ii) **Chapter III** contains an account on the systematic procedure undertaken to study these events. At the very beginning the criteria of selecting the detectors to carry out the present kind of study is discussed. Thereafter, preparation of detectors and their irradiations to specific projectiles are described in detail. In section III.3 the chemical processing of the detectors in suitable chemical reagents have been dealt with and in the next section an account on the observation and scanning of the processed detectors is given where the measurement of different parameters of an event are discussed along with the determination of energy of the projectile, the track density and detector calibrations. This chapter is concluded by a detail account on the error analysis.

(iii) **Chapter IV** contains a systematic account of the experimental results and related discussions under the following sub-heads: statistics of events, differential and total cross-sections, total mass of fragments, the Q-Values of the nuclear reactions, relative velocity of fragments, the opening angle in the laboratory and centre of mass systems and the results obtained from the

systematic analysis carried out on the third prongs.

(iv) and finally in **chapter V** the significant results of the present investigation are highlighted. A brief description on the potentialities and scopes of this track technique is presented for some future applications.

(v) The source codes of the programs 'TRANSCORD' and 'HIFISS' are given in the appendices A and B respectively.